ANALYTICAL SCIENCES JULY 2017, VOL. 33

MnO_2 Nanosheet-based Fluorescence Sensing Platform for Sensitive Detection of Endonuclease

Chao HU, Xiang Juan KONG, Ru Qin YU, Ting Ting CHEN,† and Xia CHU†

State Key Laboratory of Chemo/Bio-Sensing and Chemometrics, College of Chemistry and Chemical Engineering, Hunan University, Changsha 410082, P. R. China

A novel fluorescence sensing platform for ultrasensitive detection of S1 nuclease activity has been constructed based on MnO_2 nanosheets and FAM labeled single-stranded DNA (FAM-ssDNA). In this system, MnO_2 nanosheets were found to have different adsorbent ability toward ssDNA and mono- or oligonucleotide fragments. FAM-ssDNA could adsorb on MnO_2 nanosheets and resulted in significant fluorescence quenching through fluorescence resonance energy transfer (FRET), while mono- or oligonucleotide fragments could not adsorb on MnO_2 nanosheets and still retained strong fluorescence emission. With the addition of S1 nuclease, FAM-ssDNA was cleaved into mono- or oligonucleotide fragments, which were not able to adsorb on MnO_2 nanosheets and the fluorescence signal was never quenched. The different fluorescence intensity allowed for examination of S1 nuclease activity. The developed method can detect S1 nuclease activity in the range of 0 – 20 U mL^{-1} with a detection limit of 0.05 U mL^{-1}. Benefits of the system include less time-consuming processes and more simple design compared to other endonuclease assays. Satisfactory performance for S1 nuclease in complex samples has been successfully demonstrated with the system. The developed assay could potentially provide a new platform in bioimaging and clinical diagnosis.

Keywords FAM-ssDNA, S1 nuclease, MnO_2 nanosheets, fluorescence

(Received December 22, 2016; Accepted February 10, 2017; Published July 10, 2017)

Introduction

Endonucleases are a family of nucleases that can catalyze the cleavage reactions by hydrolyzing the phosphodiester bonds of DNA or RNA into small oligonucleotide fragments. These hydrolytic reactions are involved in many important cellular biological processes, such as DNA repairing, recombination, transformation, molecular cloning, genotyping and mapping.[1-5] In view of their intrinsic biological importance, developing efficient assays for endonuclease activity is essential in the fields of molecular biology and biosensing. Many conventional analytical methods for assessing endonuclease activity have been developed, including polyacrylamide gel electrophoresis (PAGE),[6] high-performance liquid chromatography (HPLC),[7,8] radioactive labeling,[9] and enzyme-linked immunosorbent assay (ELISA).[10,11] However, most of these methods are limited by laborious, discontinuous time-consuming procedures and complex design, which restrict their widespread application. To address these challenges, recently, many electrochemical approaches[12] and copper nanoparticle-based fluorescent assays have been conducted.[13] Our group has developed an RCA-based, exonuclease III-aided recycling dual-amplication technique[14] and a DNA-silver nanocluster (DNA-AgNC) probe for detecting endonuclease.[15] Although these fluorescent methods are promising and have made great improvements in endonuclease assay, they also have drawbacks such as time-consuming and sophisticated synthesis processes. Fluorescence resonance energy transfer (FRET) is a nonradiative process that involves energy transfer from energy donors to energy acceptors in the range of 1 – 10 nm, *via* long-range dipole-dipole interactions. Owing to its simpleness coupled with fluorescence, FRET has been recognized as an appealing and sensitive method for bioanalysis. Therefore, it is meaningful to design a efficient, facile, and sensitive method based on FRET to detect endonuclease in biological samples.

In recent research, two-dimensional (2D) nanomaterials have emerged as promising nanoplatforms for biosensing due to their unique optical, electronic and mechanical properties.[16-21] The 2D nanomaterials hold fascinating characteristics such as planar structure, semiconducting and high specific surface areas, which provide for widespread applications in sensing,[22] energy generation,[23] and photocatalysis[24] *via* π–π stacking or hydrogen bonding. Besides, they have also been particularly useful in the construction of sensors due to the good light absorption capability and fast electron-transfer rate. Graphene oxide has attracted increasing attention and has been adopted for many successful applications in sensing platforms.[25-29] Another 2D material, MoS_2 nanosheets, have been used as energy acceptors, and dye-modified ssDNA designed as energy donors were also applied for the detection of biomolecules.[30] Lately, MnO_2 nanosheets have received tremendous attention and have found applications in electrochemistry, energy conversion, catalysis, and storage.[31-33] MnO_2 nanosheets with the thickness on the order of nanometers or smaller with lateral size ranging from submicrometers to micrometers are composed of an edge-shared

† To whom correspondence should be addressed.
E-mail: chenting1104@hnu.edu.cn (T. T. C.); xiachu@hnu.edu.cn (X. C.)

MnO_6 octahedral crystal lattice. The MnO_2 nanosheets have been reported as efficient quenchers, owing to the d–d transition of Mn ions in the MnO_6 octahedra. Recently, Tan *et al*. reported an MnO_2 nanosheet-aptamer nanoprobe for fluorescence/MRI bimodal tumor cell imaging based on the light absorbing property and redox activity of MnO_2 nanosheets.[34]

Herein, we developed a sensitive and selective strategy for endonuclease detection based on the MnO_2 nanosheets and 6′-carboxyfluorescein labeled single stranded DNA (FAM-ssDNA). The fluorescence of FAM-ssDNA could adsorb on MnO_2 nanosheets and be totally quenched by it through FRET, while the mono- or oligonucleotide fragments were not able to adsorb on MnO_2 nanosheets and the fluorescence signal was still retained. In this work, we chose S1 nuclease as a model enzyme. The enzyme has been used to explore the destruction of the DNA secondary structure by numerous carcinogens and can recognize DNA lesions created by bulky carcinogens.[35] With the addition of S1 nuclease, which is a widespread ssDNA specific endonuclease that hydrolyzes ssDNA into mono- or oligonucleotide fragments, the fluorescence signal was never quenched when mixed with MnO_2 nanosheets. To our knowledge, this is the first use of MnO_2 nanosheets as an effective energy acceptor of fluorescent dye to analyze the activity of important endonuclease. Compared with the previous reported methods such as the graphene oxide-based system,[36] the proposed strategy is simple, rapid and possesses satisfactory analytical performance.

Experimental

Reagents and chemicals

The 2-(*N*-morpholino) ethanesulfonic acid (MES), sodium 4-(2-hydro-xyethyl) piperazine-1-ethanesufonate (HEPES) and NaCl were purchased from Sigma-Aldrich. The S1 nuclease (100 units μL^{-1}) was purchased from Thermo Fisher Scientific Inc. The S1 nuclease buffer-2 (20 mM NaAc, 150 mM NaCl, and 1 mM $ZnSO_4$, pH 4.5) was used for S1 nuclease dilution and enzymatic digestion reaction. Exonuclease III, T4 polynucleotide kinase (10 units μL^{-1}), and λ exonuclease (5 units μL^{-1}) were obtained from New England Biolabs (NEB, UK). $KMnO_4$ was purchased from Sinopharm Chemical Reagent Co., Ltd. (Shanghai, China). RPMI 1640 cell medium was provided by Sangon Biotech Co., Ltd. (Shanghai, China). All reagents were used as received without further purification. The DNA sequences used in this work were also synthesized and HPLC purified by Sangon Biotech Co., Ltd. (Shanghai, China), and the sequence was listed as follows: 5′-FAM-AAA AAA AAA TCT AAC TGC TGC GCC GCC GGG AAA ATA CTG TAC GGT TAG A-3′. S1 nuclease degrades single-stranded DNA of which the sequence has no effect on the process.[37] MnO_2 nanosheets exhibited a high quenching efficacy on FAM-ssDNA, which increased with the increase of base number and could reach almost 98% for 49-base ssDNA that was used here according to the literature of Tan *et al*.[34] All solutions were prepared using ultrapure water, which was prepared through a Millipore Milli-Q water purification system (Billerica, USA) and electric resistance >18.2 M.

Apparatus

The fluorescence spectra were measured using an FL-7000 spectrometer (Hitachi, Japan). The excitation wavelength was fixed at 480 nm with a recording emission range from 500 to 600 nm and the excitation and emission slits were set at 5 nm, with a 900-V PMT voltage. The UV-vis absorption spectrum was acquired from a UV-2450 UV-visible spectrometer (Shimadzu, Japan). The transmission electron microscopy (TEM) images were collected on a field emission high resolution 2100 F TEM (JEOL, Japan) operating at an acceleration voltage of 200 kV.

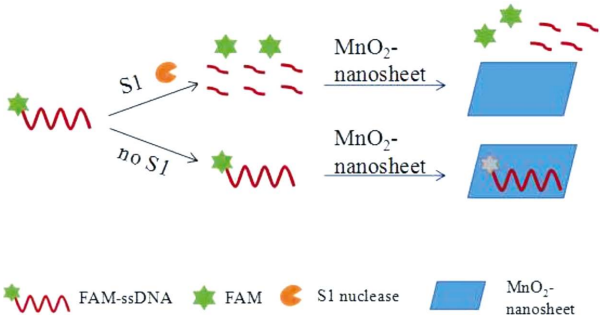

Scheme 1 Schematic illustration of MnO_2 nanosheet-based fluorescence sensing platform for the analysis of S1 nuclease activity.

Preparation of MnO_2 nanosheets

MnO_2 nanosheets were synthesized as reported previously with slight modification.[38] A 2-mL microcentrifuge tube containing 10 mM $KMnO_4$ 450 µL and 0.1 M MES buffer 600 µL (pH 6.0) was sonicated for 30 min until a brown colloid was formed. Then the solution was centrifuged at 5000 rpm for 5 min to collect the precipitate, washed with deionized water several times and redispersed in 1 mL of deionized water with the concentration of about 1.0 mg mL^{-1}.

Preparation of FAM-ssDNA fluorescence quenching assay

To evaluate the fluorescence quenching of FAM-ssDNA on the MnO_2 nanosheets surface, 100 nM FAM-ssDNA was prepared in the reaction buffer-1 (20 mM Hepes, 150 mM NaCl, pH 9.0). After the addition of different amounts of MnO_2 nanosheets (1.0 mg mL^{-1}), the solution was mixed well and incubated for another 10 min at room temperature. Then, the fluorescence emission spectra were recorded with an excitation wavelength of 480 nm.

Procedure for the S1 nuclease activity assay

A 20-µL aliquot of reaction solution containing 0.5 µM FAM-ssDNA, S1 nuclease buffer-2 and S1 nuclease of various concentrations was incubated at 37°C for 50 min. Then the above mixture was heated at 95°C for 5 min to terminate the cleavage reaction. A solution of MnO_2 nanosheets (50 µg mL^{-1}) and buffer-1 were added to yield a total volume of 100 µL. After reaction at room temperature for 10 min, the fluorescence emission spectra were recorded.

Results and Discussion

Strategy for S1 nuclease activity analysis

Taking advantage of the characteristics of the MnO_2 nanosheets, a novel fluorescent method for S1 nuclease assay was proposed in this work. The sensing mechanisms of S1 nuclease activity are shown in Scheme 1. In the absence of S1 nuclease, the FAM labeled ssDNA could be adsorbed on the surface of MnO_2 nanosheets *via* π-π stacking interaction, which results in consideraber fluorescence suppressing because of the effective FRET between fluorescent dye and MnO_2 nanosheets.

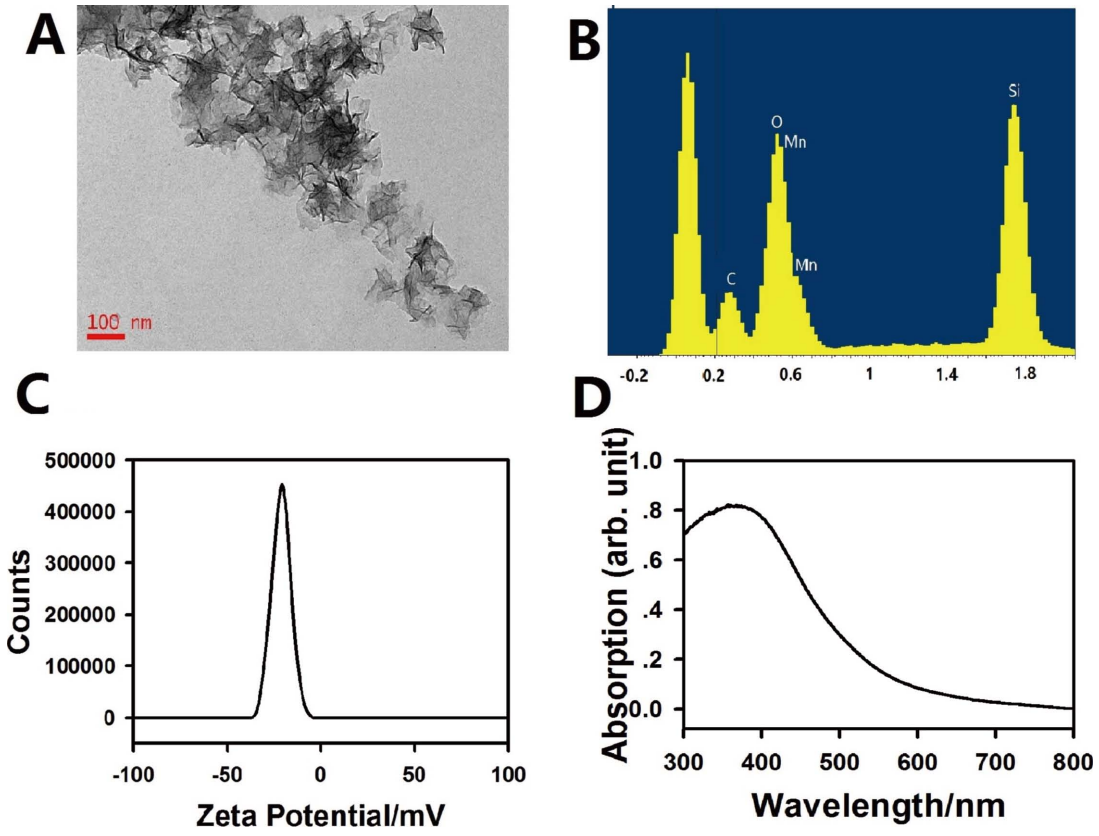

Fig. 1 (A) TEM image of MnO_2 nanosheets. Scale bar: 100 nm. (B) Energy dispersive X-ray spectroscope (EDS) spectra of MnO_2 nanosheets. (C) Zeta potential of MnO_2 nanosheets at 60 μg mL^{-1}. (D) UV-vis absorption spectrum of MnO_2 nanosheets.

In the presence of S1 nuclease, however, the ssDNA cleavage reaction was triggered, resulting in mono- or oligonucleotide fragments, which led to the FAM release from ssDNA and failure to adsorb on the surface of MnO_2 nanosheets. This resulted in the restoration of fluorescence. Therefore, the proposed method could be applied to detect S1 nuclease.

Characterization of MnO_2 nanosheets

The synthesized MnO_2 nanosheets were characterized by transmission electron microscope (TEM), energy dispersive X-ray spectroscope (EDS), ζ potential and UV-vis absorption spectra. As shown in Fig. 1A, the typical nanosheet morphology of MnO_2, ultrathin plane with occasional folds, wrinkles and a large 2D, is revealed as in previous reports.[38,39] Compositional analysis of the MnO_2 nanosheets by energy dispersive X-ray spectroscope (EDS) measurement showed the signals of Mn and O elements (Fig. 1B). The ζ potential of the MnO_2 nanosheets was measured to be about –22.1 V at 60 μg mL^{-1} (Fig. 1C), indicating a negative charge on the MnO_2 nanosheet surfaces. The MnO_2 nanosheets prepared here exhibited a wide absorption band ranging from 300 to 600 nm with an absorption peak at 380 nm (Fig. 1D), which indicated that the MnO_2 nanosheets have wide absorption and might serve as an efficient quencher to the fluorescence group.

Performance of the strategy

To verify the application of our strategy for detecting endonuclease, fluorescence measurements were investigated. Upon being excited at 480 nm, FAM labeled ssDNA (100 nM) emitted strong fluorescence around 525 nm in the absence of

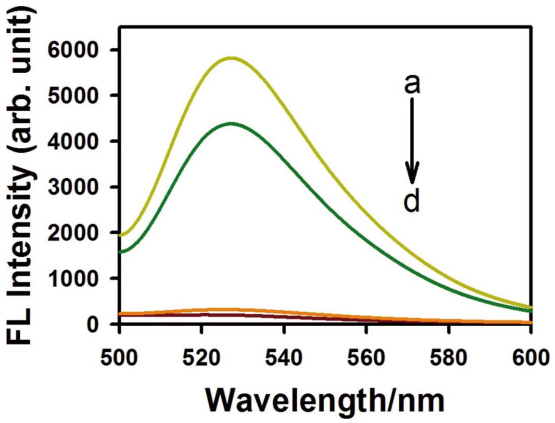

Fig. 2 Fluorescence intensity of 100 nM FAM-ssDNA under different conditions: (a) only FAM-ssDNA; (b) with MnO_2 nanosheets and 10 U mL^{-1} S1 nuclease; (c) with MnO_2 nanosheets; (d) with MnO_2 nanosheets and denatured 10 U mL^{-1} S1 nuclease.

MnO_2 nanosheets, as shown in Fig. 2a. However, the fluorescence emission decreased dramatically upon addition of MnO_2 nanosheets at 50 μg mL^{-1} (Fig. 2c). These results confirmed that the MnO_2 nanosheets can efficiently quench fluorescence as the results of the strong absorption of fluorophore labeled ssDNA on the MnO_2 nanosheet surface and effective FRET between the fluorescent dye and MnO_2 nanosheets. By contrast, in the presence of S1 nuclease, the reaction solution

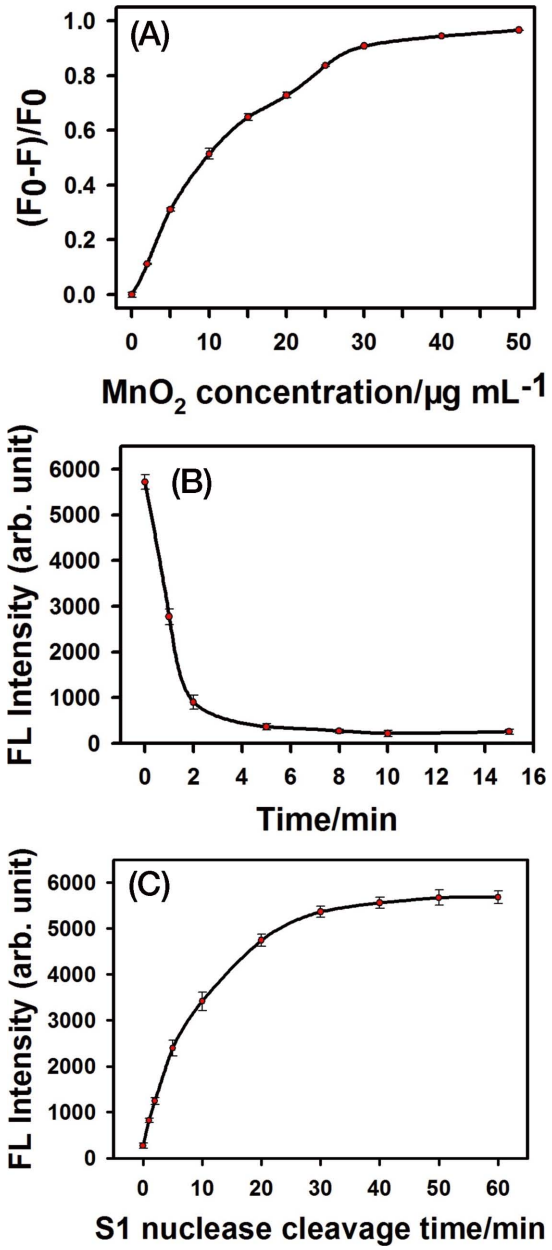

Fig. 3 (A) The $(F_0 - F)/F_0$ as a function of MnO_2 nanosheet concentration. F_0 and F were the fluorescence intensities without and with MnO_2 nanosheets, respectively. (B) Relationship of the fluorescence intensity and reaction time. (C) Fluorescence intensity changes of FAM-ssDNA as a function of S1 nuclease-catalyzed cleavage time.

showed a high fluorescence response when was added the same concentration of MnO_2 nanosheets (Fig. 2b). The result indicated that the FAM-ssDNA was cleaved into mono- or oligonucleotide fragments, yielding weak absorption between fluorecent dye and MnO_2 nanosheets. We aimed to validate whether the S1 nuclease itself had an effect on the fluorescence of FAM labeled ssDNA. S1 nuclease was first inactivated through heating at 95°C for 5 min, then incubated with FAM-ssDNA, instead of the active S1 nuclease. The resulting solution showed low fluorescence (Fig. 2d), leading us to conclude that the fluorescence change was owing to the cleavage reaction of FAM-ssDNA by S1 nuclease.

Optimization of reaction condition

In order to achieve an excellent signal response, we investigated the fluorescence responses of FAM-ssDNA under different concentrations of MnO_2 nanosheets. The fluorescence intensity of FAM-ssDNA at 525 nm was gradually quenched with the increasing concentration of MnO_2 nanosheets (Fig. 3A). Figure 3A shows the observed quenching efficiency of MnO_2 nanosheets, which was defined as $(F_0 - F)/F_0$ (F_0 and F were the fluorescence intensities without and with MnO_2 nanosheets, respectively). We found that the maximum quenching efficiency of MnO_2 nanosheets reached up to 96% and the maximal value was 50 μg mL^{-1} MnO_2 nanosheets. Such results are mainly attributed to the strong and stable adsorption of ssDNA on the MnO_2 nanosheet surfaces, resulting in the occurrence of FRET. Thus, 50 μg mL^{-1} was used in the following experiments for MnO_2 nanosheets. The reaction time of FAM-ssDNA and MnO_2 nanosheets was a critical parameter. The fluorescence intensity decreased rapidly when in the presence of MnO_2 nanosheets as incubation time increased, and then reached equilibrium after 10 min, suggesting complete adsorption and FRET (Fig. 3B). Therefore, 10 min was chosen in the subsequent experiments. As shown in Fig. 3C, the fluorescence intensity, showing dynamic monitoring of the ssDNA digestion reaction, was affected by the cleavage time of S1 nuclease. During the cleavage time from 0 to 50 min, the emission maximum of FAM-ssDNA at 525 nm increased gradually. The fluorescence quickly increased in the first 20 min, but then no changes were observed after 50 min. It was determined that the FAM-ssDNA cleaves completely within 50 min, thus, 50 min was chosen as the S1 nuclease-catalyzed cleavage time.

Assay of S1 nuclease activity

To achieve the dynamic response range and detectable minimum concentration of endonuclease by our strategy, the fluorescence responses at different amounts of S1 nuclease under the optimized experimental condition are plotted in Fig. 4A. It observed that the fluorescence intensity continually increased with increasing concentration of S1 nuclease from 0 to 20 U mL^{-1}, indicating a gradual cleavage reaction of FAM-ssDNA. Compared with the graphene oxide-based system,[39] our developed method extends the detection range. A good regression coefficient ($R^2 = 0.988$) to the S1 nuclease concentration is raised from 0.1 to 3 U mL^{-1} (Fig. 4B). Moreover, it should be highlighted that according to the 3σ rule, 0.05 U mL^{-1} S1 nuclease can be detected. The result proposes that the MnO_2 nanosheets based on this fluorescence sensing platform could be used for sensitive detection of S1 nuclease.

Specificity of the assay

To examine the specificity of the MnO_2 nanosheet-based nanoprobe for S1 nuclease, T4 polynucleotide kinase (T4 PNK), λ exonuclease (λ exo), exonuclease III (Exo III) and acetylcholinesterase (AchE) were added into the sensing system instead of S1 nuclease to investigate the specificity. As shown in Fig. 5, only S1 nuclease caused a high fluorescence response, and no meaningful differences were detected between the blank after addition of other analogs. These results clearly demonstrated that the proposed method was specific for S1 nuclease by taking advantage of the cleavage reaction.

Determination of S1 nuclease activity in complex samples

To explore the feasibility of the MnO_2 nanosheet-based nanoprobe for S1 nuclease determination, the proposed method was applied to the RPMI 1640 cell medium samples. The recovery experiment was carried out in 5% (v/v) RPMI 1640

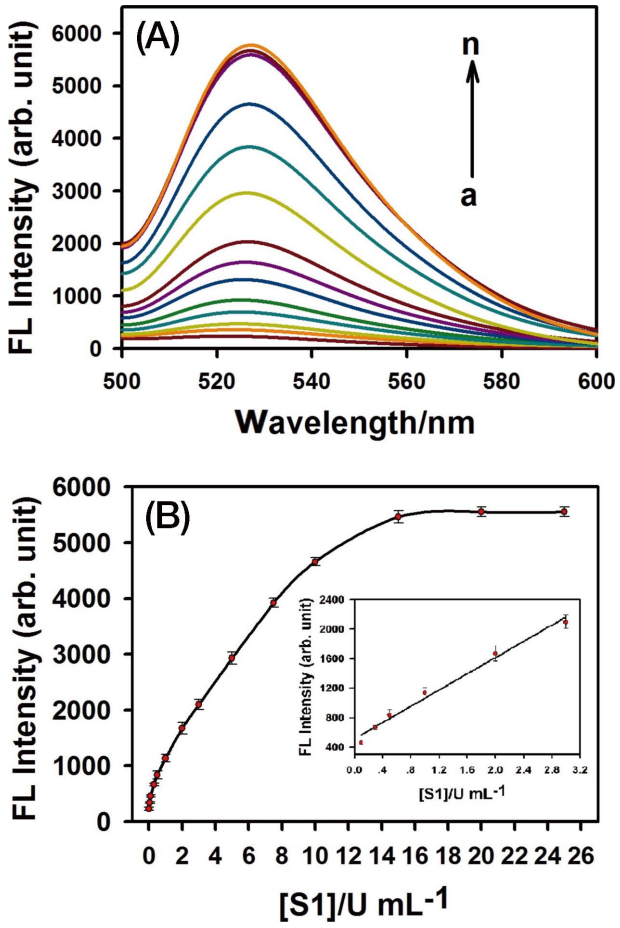

Fig. 4 (A) Fluorescence intensity with varying concentrations of S1 nuclease (top to bottom, 0, 0.05, 0.1, 0.3, 0.5, 1.0, 2.0, 3.0, 5.0, 7.5, 10, 15, 20, 25 U mL^{-1}) in reaction buffer. (B) Relationship between the fluorescence intensity of MnO_2 nanosheets and S1 nuclease. Inset shows the linear response of the assay system to S1 nuclease. Error bars represent standard deviations from three repeated experiments.

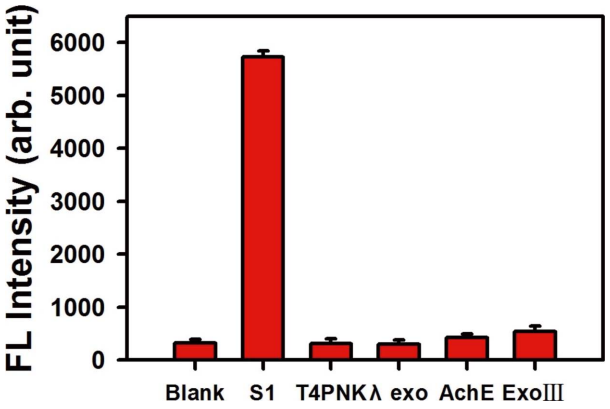

Fig. 5 Selectivity analysis of the assay system. S1 nuclease concentration was 20 U mL^{-1}. The concentration of other analytes was 50 U mL^{-1}. Error bars represent standard deviations from three repeated experiments.

Table 1 Determination of S1 nuclease activity from RPMI 1640 Cell Medium

Added/U mL^{-1}	Found/U mL^{-1}	Recovery	RSD, % (n = 3)
2.0	1.92	96	4.7
4.0	3.76	94	5.2
10	10.4	104	6.1

cell medium samples,[40] and the results are displayed in Table 1. The recoveries and RSD for different concentrations of S1 were satisfactory, indicating that the method was acceptable and practical in complex biological samples.

Conclusions

In conclusion, we succeeded in demonstrating a novel fluorescence sensing platform based on MnO_2 nanosheets for ultrasensitive detection of S1 nuclease activity. To the best of our knowledge, this is the first use of MnO_2 nanosheets to detect endonuclease. Owing to the adsorbent ability of MnO_2 nanosheets, a fine signal-to-background and selective sensing assay with favorable performance for S1 nuclease in complex samples has been successfully developed. In addition, this method does not require the time-consuming processes and complex design of other endonuclease assays. Furthermore, the developed assay could potentially provide a new platform for bioimaging and clinical diagnosis.

Acknowledgements

This work was supported by the National Natural Science Foundation of China (No. 21525522 and 21275045).

References

1. N. D. F. Grindley, K. L. Whiteson, and P. A. Rice, *Annu. Rev. Biochem.*, **2006**, *75*, 567.
2. M. R. Lieber, *BioEssays*, **1997**, *19*, 233.
3. T. M. Marti and O. Fleck, *Cell. Mol. Life Sci.*, **2004**, *61*, 336.
4. P. Norberg, T. Bergstrom, and J. A. Liljeqvist, *J. Clin. Microbiol.*, **2006**, *44*, 4511.
5. S. C. West, *Nat. Rev. Mol. Cell Biol.*, **2003**, *4*, 435.
6. A. L. Rosenthal and S. A. Lacks, *Anal. Biochem.*, **1977**, *80*, 76.
7. S. Spitzer and F. Eckstein, *Nucleic Acids Res.*, **1988**, *16*, 11691.
8. L. W. McLaughlin, F. Benseler, E. Graeser, N. Piel, and S. Scholtissek, *Biochemistry*, **1987**, *26*, 7238.
9. S. Halford and A. Goodall, *Biochemistry*, **1988**, *27*, 1771.
10. A. Jeltsch, A. Fritz, J. Alves, H. Wolfes, and A. Pingoud, *Anal. Biochem.*, **1993**, *213*, 234.
11. K. Hiramatsu, H. Miura, S. Kamei, K. Iwasaki, and M. Kawakita, *J. Biochem.*, **1998**, *124*, 231.
12. T. Li, S. Dong, and E. Wang, *Anal. Chem.*, **2009**, *81*, 2144.
13. Z. H. Qing, X. X. He, T. P. Qing, K. M. Wang, S. Hui, D. G. He, Z. Zou, L. Yan, F. Z. Xu, X. S. Ye, and Z. G. Mao, *Anal. Chem.*, **2013**, *85*, 12138.
14. C. L. Liu, X. J. Kong, J. Yuan, R. Q. Yu, and X. Chu, *RSC Adv.*, **2015**, *5*, 75055.

15. X. Tian, X. J. Kong, Z. M. Zhu, T. T. Chen, and X. Chu, *Talanta*, **2015**, *131*, 116.
16. D. Chen, H. B. Feng, and J. H. Li, *Chem. Rev.*, **2012**, *112*, 6027.
17. L. H. Tang, Y. Wang, Y. Liu, and J. H. Li, *ACS Nano*, **2011**, *5*, 3817.
18. X. Huang, Z. Y. Zeng, and H. Zhang, *Chem. Soc. Rev.*, **2013**, *42*, 1934.
19. S. J. Guo and S. J. Dong, *Chem. Soc. Rev.*, **2011**, *40*, 2644.
20. H. Zhang, *ACS Nano*, **2015**, *9*, 9451.
21. C. L. Tan and H. Zhang, *Chem. Soc. Rev.*, **2015**, *44*, 2713.
22. M. Pumera and A. H. Loo, *Anal. Chem.*, **2014**, *61*, 49.
23. D. Merki, S. Fierro, H. Vrubel, and X. L. Hu, *Chem. Sci.*, **2011**, *2*, 1262.
24. Q. Li, N. Zhang, Y. Yang, G. Wang, and D. H. Dg, *Langmuir*, **2014**, *30*, 8965.
25. Y. Wang, L. H. Tang, Z. H. Li, Y. H. Lin, and J. H. Li, *Nat. Protocol*, **2014**, *9*, 1944.
26. C. H. Lu, H. H. Yang, C. L. Zhu, X. Chen, and G. N. Chen, *Angew. Chem., Int. Ed.*, **2009**, *48*, 4785.
27. J. J. Xu, W. W. Zhao, S. P. Song, C. H. Fan, and H. Y. Chen, *Chem. Soc. Rev.*, **2014**, *43*, 1601.
28. B. W. Liu, Z. Y. Sun, X. Zhang, and J. W. Liu, *Anal. Chem.*, **2013**, *85*, 7987.
29. X. H. Cao, Z. Y. Yin, and H. Zhang, *Energ. Environ. Sci.*, **2014**, *7*, 1850.
30. C. F. Zhu, Z. Y. Zeng, H. Li, F. Li, C. H. Fan, and H. Zhang, *J. Am. Chem. Soc.*, **2013**, *135*, 5998.
31. L. L. Peng, X. Peng, B. R. Liu, C. Z. Wu, Y. Xie, and G. H. Yu, *Nano Lett.*, **2013**, *13*, 2151.
32. M. Toupin, T. Brousse, and D. Bélanger, *Chem. Mater.*, **2004**, *16*, 3184.
33. S. H. Yang, X. F. Song, P. Zhang, and L. Gao, *ACS Appl. Mater. Interfaces*, **2013**, *5*, 3317.
34. Z. L. Zhao, H. H. Fan, G. F. Zhou, H. R. Bai, H. Liang, R. W. Wang, X. B. Zhang, and W. H. Tan, *J. Am. Chem. Soc.*, **2014**, *136*, 11220.
35. S. Galiegue, B. Bailleul, M. H. Loucheux-Lefebvre, and J. Laval, *Carcinogenesis*, **1982**, *3*, 435.
36. Y. He, B. N. Jiao, and H. W. Tang, *RSC Adv.*, **2014**, *4*, 18294.
37. V. M. Vogt, *Eur. J. Biochem.*, **1973**, *33*, 192.
38. J. Yuan, Y. Cen, X. J. Kong, S. Wu, C. L. W. Liu, R. Q. Yu, and X. Chu, *ACS Appl. Mater. Interfaces*, **2015**, *7*, 10548.
39. R. R. Deng, X. J. Xie, M. Vendrell, Y. T. Chang, and X. G. Liu, *J. Am. Chem. Soc.*, **2011**, *133*, 20168.
40. L. J. Huang, X. Tian, J. T. Yi, R. Q. Yu, and X. Chu, *Anal. Methods*, **2015**, *7*, 7474.